Journal of Electroanalytical Chemistry 756 (2015) 77–83

Contents lists available at ScienceDirect

Journal of Electroanalytical Chemistry

journal homepage: www.elsevier.com/locate/jeac

Assembly of magnetic nanoparticles at a liquid/liquid interface. Catalytic effect on ion transfer process

C.I. Cámara [a], L.M.A. Monzón [b,*], J.M.D. Coey [b], L.M. Yudi [a,*]

[a] INFIQC (CONICET-Universidad Nacional de Córdoba). Departamento de Fisicoquímica, Facultad de Ciencias Químicas, Ala 1, Pabellón Argentina, Ciudad Universitaria, 5000 Córdoba, Argentina
[b] School of Physics, SNIAMS Building, Trinity College Dublin, Dublin 2, Ireland

ARTICLE INFO

Article history:
Received 16 February 2015
Received in revised form 4 June 2015
Accepted 30 June 2015
Available online 9 August 2015

Keywords:
Magnetic nanoparticles
Films
Self-assembly
Liquid/liquid interfaces
Electrochemistry

ABSTRACT

The adsorption of cobalt (Co) and cobalt–boron (Co_xB) magnetic nanoparticles (NPs) at a liquid/liquid interface is examined. The Co NPs have a remanent magnetization while the Co_xB is completely demagnetized in the absence of an external magnetic field. Cyclic voltammetry experiments reveal that the adsorption of these NPs at the interface shifts the positive potential limit toward lower values showing that a catalytic effect on the ion transfer process is occurring, while electrochemical impedance spectroscopy demonstrates that their mode of self-assembly is directed by their magnetic properties. Co_xB NPs form a homogeneous film while Co segregates in macroscopic patches, leaving some areas of the interface uncovered.

1. Introduction

The growing interest in ferromagnetic nanoparticles (NPs) is largely motivated to their wide applications in biomedicine [1,2] and biotechnology [3]. They are similar in size to biomolecules [4] and the most common applications in biomedicine are in magnetic resonance imaging [4], drug delivery [5] and hyperthermia cancer therapies [1,6]. Due to their unique properties originating from their small size and large surface area, such as their easy penetration of biomembrane systems, successful strategies to generate biofunctional magnetic nanoparticles for application in protein and pathogen detection have been reported [7].

In the last two decades several kinds of nanoparticle films have been generated at polarized liquid/liquid interfaces. These studies focused on the synthesis, characterization and applications of gold [8,9], platinum [10,11], palladium [11–13], silver [14] and Au–Pd core–shell [9] nanoparticles, demonstrating that the polarization allows us to control the size of the nanoparticles as well as manipulate them [13]. On the other hand, the Langmuir–Schaefer technique has been applied to prepare two-dimensional super paramagnetic films of tridodecylamine-stabilized Co nanoparticles [15]. However, no studies have yet reported the interfacial behavior of magnetic NPs on polarized liquid/liquid interfaces. In the present paper we first characterize the adsorption of Co and Co_xB NPs at these interfaces using cyclic voltammetry (CV) and electrochemical impedance spectroscopy (EIS), complemented with magnetic studies, scanning electron microscopy (SEM), Fourier transform infrared spectroscopy (FT-IR) and energy dispersive X-ray spectroscopy (EDS). The importance of this study is based on the similarity of the water/organic solvent interface with that generated at the cell membrane in the extra-cellular environment [16,17].

2. Materials and methods

CV and EIS were used to characterize the film of NPs at the liquid/liquid interface, using a conventional glass cell (0.94 cm^2 interfacial area) with a four-electrode configuration [17]. Two platinum wires were employed as counter electrodes and the reference electrodes were Ag/AgCl. The reference electrode in contact with the organic solution was immersed in an aqueous solution of 10.0 mM tetraphenylarsonium chloride (TPAsCl, Aldrich). Potential values (E) reported in this work are those which include $\Delta\phi^0_{tr,\ TPAs+} = 0.364$ V for the transfer of the ion $TPAs^+$.

The supporting electrolyte solutions were 10.0 mM $CaCl_2$ (p.a. grade) in ultra-pure water and 10.0 mM tetraphenylarsonium tetrakis (4-chloro phenyl) borate (TPhAsTClPhB) in 1,2-dichloroethane (1,2-DCE, Dorwill p.a.). The pH of the aqueous solution was 5.00. TPhAsTClPhB was prepared by metathesis of tetraphenylarsonium chloride (TPhAsCl, Sigma-Aldrich) and potassium tetrakis (4-chloro phenyl) borate (KTClPhB, Aldrich p.a.).

* Corresponding authors.
E-mail addresses: aranzazl@tcd.ie (L.M.A. Monzón), mjudi@fcq.unc.edu.ar (L.M. Yudi).

http://dx.doi.org/10.1016/j.jelechem.2015.06.020
1572-6657/

The electrochemical cell used was as follows:

Ag	AgCl	TPhAsCl 10.0 mM (w′)	TPhAsTClPhB 10.0 mM (o)	$CaCl_2$ 10.0 mM (pH = 5.00) (w)	AgCl	Ag

Co and Co_xB NPs were prepared according to general protocols [18]. Particularly Co NPs were synthesized employing 9.00 mL of dioctylether (Sigma-Aldrich), 0.50 mL of oleic acid (Sigma-Aldrich) and 0.20 mL of oley amine (Sigma-Aldrich). The mixture was agitated at 80 °C during 1 h, under Ar. Then 0.0470 g $CoCl_2$ was added under constant agitation at T = 150 °C. After dissolution of the salt, 2.00 mL of lithium triethylborohydride ($LiEt_3BH$, Sigma-Aldrich) was injected and temperature was increased to 200 °C during 30 min. Later, the mixture was allowed to stand during 2 h at room temperature and then ethanol was added to precipitate Co NPs, which were separated and washed with acetone.

Co_xB NPs were synthesized dissolving 0.4300 g of $CoCl_2$ and 0.0860 g of sodium butanoate (Sigma-Aldrich) in aqueous/ethanol solution, under stirring at 60 °C. After dissolution, 0.1200 g of $NaBH_4$ was incorporated. The resulting mixture was allowed to stand during 30 min at room temperature. Then Co_xB NPs were magnetically separated from the solution and washed several times.

The NPs dispersion was prepared in ethyl alcohol, at a concentration 0.73 g/mL. It was sonicated for 10 min before use and injected into the 1,2-DCE organic phase, close to the interface. CV and EIS experiments were performed at room temperature 30 min after injection.

CV was performed using a potentiostat with periodic current interruption, for automatic elimination of solution resistance, and a potential sweep generator (LyP Electrónica Argentina). EIS was carried out employing a CHI C700 electrochemical analyzer. The data acquisition and processing were made with a ZPlot/Zview (Scribner Associates Inc.) program. The frequency range was 0.05–4000 Hz, the amplitude of the *ac* perturbation was 10 mV and the constant *dc* potential, *E*, was 0.450 V. Magnetization experiments were performed on a Quantum Desing SQUID 5T magnetometer at room temperature, FT-IR spectra were recorded on a Bruker IFS28 spectrophotometer, SEM images were taken on a Zeiss Auriga microscopy and EDS measurement were made on a Carl Zeiss microscope FE-SEM Σigma. A PANalytical X'pert Pro X-ray diffractometry (XRD) system with a Cu Kα (λ = 1514.1 pm) X-ray source and an X'celerator IP detector was used to characterize the crystal structure of the nanoparticles.

3. Result and discussion

3.1. General characterization of MNPs

The characterization of MNPs was carried out employing different techniques for different purposes: magnetization curves were obtained for the evaluation of the magnetic properties of Co and C_xB NPs, XRD experiments were performed to analyze the crystal structure of both MNPs, while EDS and FT-IR experiments allowed the characterization of the NPs composition including the surfactants adsorbed on the NPs' surface.

Fig. 1 shows the magnetizations loops for Co and Co_xB NPs as a function of the applied magnetic field. The saturation magnetizations (M_s) were 45 $A \cdot m^2 \cdot kg^{-1}$ and 30 $A \cdot m^2 \cdot kg^{-1}$ for Co and Co_xB, respectively. The main difference between the samples is their coercivity, $\mu_0 H_0$ = 25 mT for Co NPs and 2 mT for Co_xB (see Fig. 1, inset), which means that the Co NPs are still magnetized when the external magnetic field is switched off, while the Co_xB NPs are not (Co NPs remaining value, M_r, is 28% of M_s). The saturation magnetization of both samples is reduced from its bulk value mainly by the oxidization of the surface and due to the B and C contents.

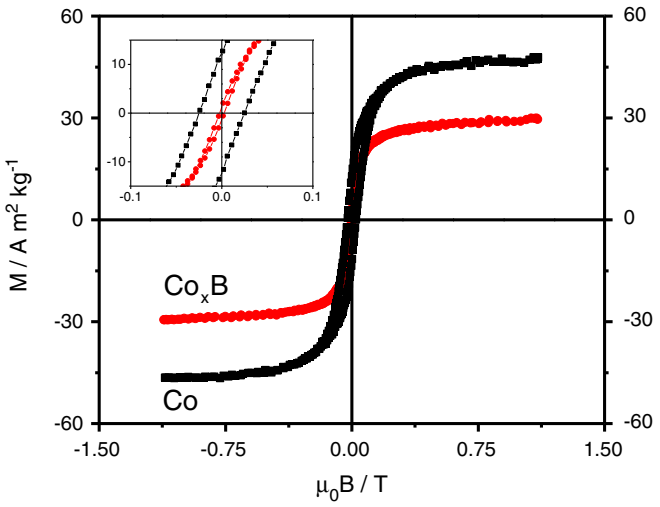

Fig. 1. Magnetic hysteresis loops for Co and Co_xB NPs. The inset shows a magnification near zero-field.

Fig. 2 shows XRD patterns of both types of magnetic nanoparticles. The data in red corresponds to Co_xB and the one shown in black to Co. There are clear differences in their crystal structures for these two types of samples: the pattern of Co_xB is typical of amorphous solids as there are no reflections that can be clearly distinguished whereas Co presents several reflections arising from the (100), (002), (101), (102), (110) and (112) planes of its hexagonal structure. For randomly oriented hcp Co powders, the intensity of the 101 reflection is much stronger than the intensity of the (002) or (100), whereas here the XRD pattern of Co nanopowder shows that the peak corresponding to the (002) reflection has a much stronger intensity than the rest. This indicates that the Co nanoparticles have a preferential orientation along the c-axis driven by the magnetocrystalline anisotropy of hcp Co. The observed room temperature coercivity of these samples suggests the existence of hcp cobalt.

Co NPs exhibit an elongated structure with an average crystal size of 25 nm (standard deviations σ = 12%) while the average size of amorphous Co_xB NPs is 30 nm (standard deviations σ = 15%). Given the non-zero magnetization of Co NPs, during the synthesis, they tend to

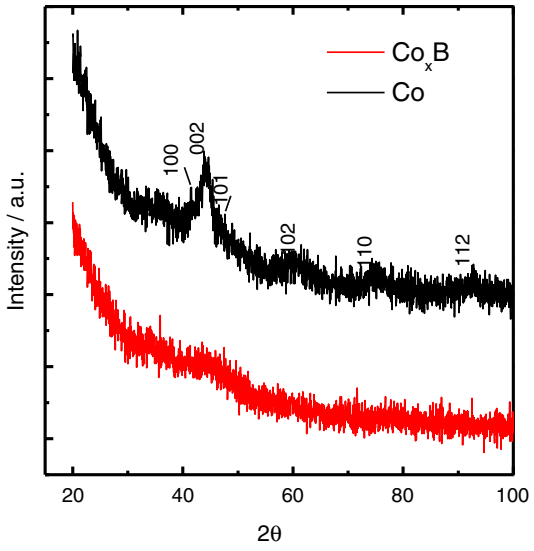

Fig. 2. XRD patterns for Co (▬) and Co_xB (▬) NPs.